QoE-Driven Resource Allocation for D2D Underlaying NOMA Cellular Networks

Liangyu Chen[†], Bo Hu[†], Shanzhi Chen[*], Guixian Xu[‡], and Jianpeng Xu[§]
[†]State Key Laboratory of Networking and Switching Technology, Beijing University of Posts and Telecommunications, Beijing 100876, China
[*]State Key Laboratory of Wireless Mobile Communications, China Academy of Telecommunication Technology, Beijing 100191, China
[‡]Department of Electrical Engineering, Tampere University, Tampere 33720, Finland
[§]State Key Laboratory of Rail Traffic Control and Safety, Beijing Jiaotong University, Beijing 100044, China
Corresponding Author: Bo Hu, hubo@bupt.edu.cn

***Abstract*—Device-to-device (D2D) communication can significantly improve network coverage and spectral efficiency. Meanwhile, non-orthogonal multiple access (NOMA) has recently been integrated with D2D communication to further improve connection density and satisfy explosive data rate requirements of end users. Considering quality of experience (QoE) has become an important indicator from the user perspective, in this paper, we study the QoE-driven resource allocation problem in a device-to-device (D2D) underlaying NOMA cellular network coexisting with D2D pairs and NOMA-based cellular users (CUs). Our target is to maximize the sum mean opinion scores (MOSs) of all users while guaranteeing the minimum QoE requirement of each CU and D2D pair, by jointly optimizing subchannel assignment and power allocation at CUs and D2D pairs. Since this problem is mixed-integer and non-convex, we first transform it into an equivalent yet more tractable form. Then, a two-stage iterative algorithm based on the alternating optimization framework and constrained concave-convex procedure technique is proposed to optimize subchannel assignment and power allocation alternately. Simulation results show that the proposed scheme outperforms the orthogonal multiple access solution and three NOMA based benchmark schemes in terms of QoE performance.**

***Index Terms*—QoE, D2D, NOMA, subchannel assignment, power allocation.**

I. Introduction

Device-to-device (D2D) communication has been regarded as an appealing solution to cope with explore traffic data demands and provide better user experience [1]. Particularly, the D2D underlaying cellular network has become a promising network architecture and has received significant attention recently. Different from the traditional cellular network, D2D underlaying cellular network allows adjacent users to communicate directly without the aid of base station (BS). Meanwhile, it also allows D2D users to reuse the frequency occupied by cellular users, which leads to spectral efficiency enhancement. In order to further improve spectral efficiency and accommodate massive connectivity of end users, non-orthogonal multiple access (NOMA) [2], [3], which allows multiple user signals coexisting in power domain or code domain, has been integrated with the D2D communication recently [4]–[7]. Compared with the conventional orthogonal multiple access (OMA) counterparts, NOMA allows more than one user to share the same time-frequency resource by applying superposition coding (SC) at transmitter and successive interference cancellation (SIC) at receiver. As a result, both spectrum efficiency and connection density can be greatly improved. Hence, making use of NOMA to serve users in the D2D underlaying cellular networks could be more attractive compared to adopting multiple sets of channels owing to constrained time-frequency resource.

While several recent works have been conducted on D2D underlaying NOMA cellular network to improve the system performance from different perspectives, such as network throughput [4]–[6], energy efficiency [7], etc, the aforementioned works in [4]–[7] mainly focus on optimizing the network's quality of service (QoS) metrics rather than the perceived quality from the user perspective. Motivated by the demands of high-quality video applications, Quality of Experience (QoE) has become one of the essential criteria of future wireless network. QoE is the end user's subjective assessment for multimedia services. In order to provide personalized and customized services for CUs and D2D users (DUs) according to their preferences in D2D underlaying NOMA cellular network, it is necessary for service and network operators to provide a high QoE for each service user through efficient resource allocation in the resource-limited wireless network.

To the best of our knowledge, the QoE-driven power and subchannel allocation has not been well investigated for D2D underlaying NOMA cellular network. Therefore, in this paper, we study the QoE-driven power and subchannel allocation to maximize the sum mean opinion scores (MOSs) of all users in D2D underlaying NOMA cellular network, while taking into account the minimum QoE constraint of each CU and DU. The considered resource allocation problem is mixed-integer and non-convex. For tractability purpose, a series of transformations are employed to convert the problem into a solvable and tractable one. Furthermore, an iterative two-stage optimization algorithm is proposed to address the converted optimization problem by leveraging alternating optimization (AO) framework and constrained concave-convex procedure

(CCCP) technique. Numerical results reveal that the proposed schemes can achieve significant enhancement of QoE performance compared to the benchmark solutions.

II. System Model and Problem Formulation

A. System Model

As shown in Fig. 1, we consider a D2D-enabled downlink single cell NOMA network consisting of one base station (BS), C cellular users (CUs) and D underlaid D2D pairs. The indices for CUs and D2D pairs are represented as $\mathcal{C} = \{1,2,\cdots,C\}$ and $\mathcal{D} = \{1,2,\cdots,D\}$, respectively. The BS transmits its signals to C CUs through N subchannels (SCs), i.e., $\mathcal{N} = \{1,2,\cdots,N\}$, and each SC occupies a bandwidth of $B_n = W/N$, where W denotes the system bandwidth. By means of the power domain NOMA, we consider multiple CUs can be served at different power level over the same SC via performing superposition coding at the BS and successive interference cancellation (SIC) at the CUs. As such, the superposition symbol transmitted by the BS to CU c on SC n can be expressed by

$$x_n = \sum_{c\in\mathcal{C}} v_c^n \sqrt{p_c^n} x_c^n \tag{1}$$

where x_c^n and p_c^n are transmit signal and transmit power from the BS to CU c on SC n. v_c^n is the SC assignment indicator for CU c, namely, if SC n is assigned to CU c, $v_c^n = 1$; otherwise, $v_c^n = 0$. Furthermore, the received signal of CU c on SC n can be given by

$$y_c^n = \underbrace{h_c^n v_c^n \sqrt{p_c^n} x_c^n}_{\text{desired signal}} + \underbrace{\sum\nolimits_{l\in\mathcal{C}/c} h_c^n v_l^n \sqrt{p_l^n} x_l^n}_{\text{interference from NOMA user}} + \underbrace{\sum\nolimits_{d\in\mathcal{D}} g_{d,c}^n u_d^n \sqrt{q_d^n} x_d^n}_{\text{interference from D2D user}} + \underbrace{z_c^n}_{\text{noise}}, \tag{2}$$

where h_c^n and $g_{d,c}^n$ are channel gains from the BS to CU c on SC n and that from the transmitter of D2D pair d to CU c on SC n, respectively. x_d^n and q_d^n is transmit signal and transmit power of the transmitter of D2D pair d on SC n. u_d^n is SC assignment indicator for D2D pair d, i.e., if SC n is assigned to D2D pair d, $u_d^n = 1$; otherwise, $u_d^n = 0$. z_c^n is noise term following the distribution $\mathcal{CN}(0,\ \delta^2)$.

According to NOMA policy, for a given SC n, CU i can successfully decode and remove the interference signal from CU j ($|h_j^n| < |h_i^n|$), if CU i's received SINR for CU j's signal is larger than or equal to the received SINR of CU j for its own signal [8]. Hence, we can obtain the following SIC decoding conditions:

$$\frac{|h_i^n|^2 v_j^n p_j^n}{I_{j,NOMA}^{i,n} + I_{i,D2D}^n + \delta^2} \geq \frac{|h_j^n|^2 v_j^n p_j^n}{I_{j,NOMA}^n + I_{j,D2D}^n + \delta^2}, \tag{3}$$

where $I_{j,NOMA}^{i,n} = \sum_{|h_l^n|>|h_j^n|} |h_i^n|^2 v_l^n p_l^n$, $I_{j,NOMA}^n = \sum_{|h_l^n|>|h_j^n|} |h_j^n|^2 v_l^n p_l^n$, $I_{i,D2D}^n = \sum_{d\in\mathcal{D}} |g_{d,i}^n|^2 u_d^n q_d^n$, and $I_{j,D2D}^n = \sum_{d\in\mathcal{D}} |g_{d,j}^n|^2 u_d^n q_d^n$. Furthermore, (3) can be equivalently transformed into

$$|h_i^n|^2 (\sum_{d\in\mathcal{D}} |g_{d,j}^n|^2 u_d^n q_d^n + \delta^2) \geq |h_j^n|^2 (\sum_{d\in\mathcal{D}} |g_{d,i}^n|^2 u_d^n q_d^n + \delta^2). \tag{4}$$

Therefore, the received signal-to-interference-plus-noise ratio (SINR) for CU u to decode its own signal is expressed by

$$\gamma_c^n = \frac{|h_c^n|^2 v_c^n p_c^n}{I_{c,NOMA}^n + I_{c,D2D}^n + \delta^2}, \tag{5}$$

Note that in our considered scenario, allowing multiple D2D pairs to reuse the same SC may improve spectrum efficiency. However, it brings heavy signaling overhead and high computational complexity [4]. Hence, we assume one SC can be assigned to at most one D2D pair, namely,

$$\sum_{d\in\mathcal{D}} u_d^n \leq 1, \forall n \in \mathcal{N}. \tag{6}$$

Then, the SINR at receiver of D2D pair d over SC n can be given by

$$\gamma_d^n = \frac{|g_d^n|^2 u_d^n q_d^n}{\sum_{c=1}^{C} |h_{B,d}^n|^2 v_c^n p_c^n + \delta^2}, \tag{7}$$

where $|g_d^n|^2$ and $|h_{B,d}^n|^2$ are channel gains between the transmitter and the receiver of D2D pair d on SC n and that from the BS to the receiver of D2D pair d on SC n.

According to (5) and (7), the data rate of CU c and D2D pair d on SC n can be given by $R_c^n = B_n \log_2(1+\gamma_c^n)$ and $R_d^n = B_n \log_2(1+\gamma_d^n)$, respectively. Thus, the overall date rate of CU c and D2D pair d can be expressed as

$$R_c = \sum_{n\in\mathcal{N}} R_c^n, \forall c \in \mathcal{C}. \tag{8}$$

and

$$R_d = \sum_{n\in\mathcal{N}} R_d^n, \forall d \in \mathcal{D}. \tag{9}$$

respectively.

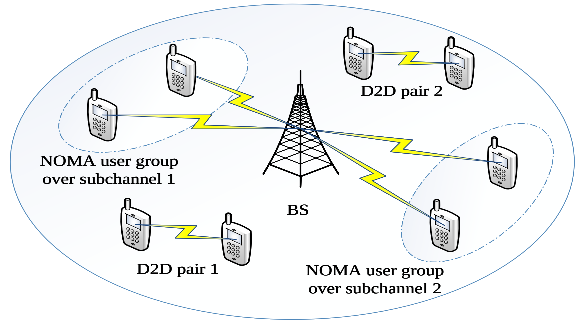

Fig. 1. The illustration of D2D underlaying NOMA cellular network.

B. QoE Evaluation Model for Web Browsing

In this paper, we use a widely adopted QoE assessment criterion named mean opinion score (MOS) to measure the perceived quality of end user experiencing real-time or interactive services. Through the MOS model, the subjective user perception for the services can be mapped to objective metrics. As one of the most popular services of wireless networks [9], this work focuses on web browsing service. The MOS model of the service can be given by [10]

$$\mathrm{MOS} = -D\ln\left(d\left(R\right)\right) + F, \tag{10}$$

where MOS_{web} value reflects the user QoE from a scale of 1 (bad) to 5 (excellent). $R\left[bit/s\right]$ represents the data rate. The constants D and F are set to be 1.1120 and 4.6746, respectively. These two parameters are designed based on the experimental analysis of web browsing. $d\left(R\right)$ represents the delay between the request for a web page and the reception of overall contents. $d\left(R\right)$ is related to the parameters including the round trip time, the web page size, and the employed protocols like Transfer Control Protocol and Hypertext Transfer Protocol. We apply these two protocols in our considered system. Thus, function $d\left(R\right)$ can be given by [9]

$$d\left(R\right) = 3RTT + \frac{FS}{R} + L\left(\frac{MSS}{R} + RTT\right) - \frac{2MSS\left(2^{L}-1\right)}{R}, \tag{11}$$

where the parameters $RTT\left[s\right]$, $MSS\left[bit\right]$ and $FS\left[bit\right]$ represent the round trip time, the maximum segment size and the web page size, respectively. $L = \min\left[L_1, L_2\right]$ is the parameter for the packet-switching cycle from user to server in the process of downloading web pages [9]), where the parameters L_1 and L_2 are given by

$$L_1 = \log_2\left(\frac{R\cdot RTT}{MSS} + 1\right) - 1,\ L_2 = \log_2\left(\frac{FS}{2MSS} + 1\right) - 1. \tag{12}$$

Note that the MOS of web browsing application has a strong sensitivity with data rate and FS, while the impact of RTT on MOS is less important especially when RTT is short range [10]. Meanwhile, as mentioned in the 3GPP technical specification of the LTE release 8, the RTT which is lower than 10 ms is expected to be achieved in future wireless networks [11]. Thus, we consider $RTT \approx 0$ ms [10] in this work and thus (11) can be reformulated as $d(R_{web}) = (FS/R_{web})$. Then, the MOS model of web browsing at the cellular user CU c and D2D pair d can be given by $\mathrm{MOS}_{CU_c} = D\ln(R_c) + C_c$ and $\mathrm{MOS}_{D2D_d} = D\ln(R_d) + C_d$, respectively, where $C_c = F - D\ln\left(FS_c\right)$ and $C_g = F - D\ln\left(FS_d\right)$ are two constants.

C. Problem Formulation

In this work, our target is to maximize the sum MOSs of all users while ensuring the minimum QoE requirement of each cellular user and D2D user. This can be achieved by jointly optimizing SC assignment and power allocation for each CU $c \in \mathcal{C}$ and D2D pair $d \in \mathcal{D}$. The considered QoE-driven resource allocation problem is formulated by

$$\max_{\left\{v_c^n, u_b^n, P_c^n, q_d^n\right\}} \sum_{c\in\mathcal{C}} \mathrm{MOS}_{CU_c} + \sum_{d\in\mathcal{D}} \mathrm{MOS}_{D2D_d} \tag{13a}$$

$$\text{s.t. } \mathrm{MOS}_{CU_c} \geq \mathrm{MOS}_{CU_c,min}, \forall c \in \mathcal{C}, \tag{13b}$$

$$\mathrm{MOS}_{D2D_d} \geq \mathrm{MOS}_{D2D_d,min}, \forall d \in \mathcal{D}, \tag{13c}$$

$$p_c^n \geq 0, \forall c \in \mathcal{C}, \forall n \in \mathcal{N};\ q_d^n \geq 0, \forall d \in \mathcal{D}, \forall n \in \mathcal{N}, \tag{13d}$$

$$\sum_{c\in\mathcal{C}}\sum_{n\in\mathcal{N}} p_c^n \leq P_{B,max};\ \sum_{n\in\mathcal{N}} q_d^n \leq P_{d,max}, \forall d \in \mathcal{D}, \tag{13e}$$

$$v_c^n \in \left\{0,1\right\}, \forall c \in \mathcal{C}, n \in \mathcal{N} \tag{13f}$$

$$\sum_{c\in\mathcal{C}} v_c^n \leq 2, \forall n \in \mathcal{N}, \tag{13g}$$

$$u_d^n \in \left\{0,1\right\}, \forall d \in \mathcal{D}, n \in \mathcal{N}, \tag{13h}$$

$$\sum_{d\in\mathcal{D}} u_d^n \leq 1, \forall n \in \mathcal{N}, \tag{13i}$$

$$(4) \tag{13j}$$

where (13b) and (13c) are the minimum MOS limitation for each CU and D2D pair to ensure the minimum user satisfaction; (13d) demonstrates the transmission power of the BS and the transmitter of each D2D pair should be positive; (13e) is the transmission power limitation of the BS and the transmitter of each D2D pair; (13f) and (13g) characterize at most two CUs can be multiplexed on each SC to reduce the decoding complexity at NOMA receiver; (13h) and (13i) mean that one SC can only be allocated to at most one D2D pair to reduce co-channel interference and signaling overhead; (13j) guarantees successful SIC at NOMA receiver. Note that (13) is a mixed-integer and non-convex problem, because i) the objective function (13a) and the constraints in (13b) and (13c) are non-convex, and ii) the constraints in (13f) and (13h) are discrete binary constraints. To tackle (13), we propose an efficient iteration approach, which will be discussed in detail in Section III.

III. Soltions To the Joint Optimization Problem

A. Problem Transformation

Since the problem (13) is non-convex and intractable, we need to transform the original optimization problem into a more tractable and solvable form. We first handle the non-convex objective function (13a). By introducing auxiliary variables $\{\eta_c\}$ and $\{\eta_d\}$, (13) can be reformulated as

$$\max_{\mathcal{Z}} \sum_{c\in\mathcal{C}} D\ln(\eta_c) + \sum_{d\in\mathcal{D}} D\ln(\eta_d) + \vartheta \tag{14a}$$

$$\text{s.t. } \sum_{n\in\mathcal{N}} R_c^n \geq \eta_c, \forall c \in \mathcal{C} \tag{14b}$$

$$\sum_{n\in\mathcal{N}} R_d^n \geq \eta_d, \forall d \in \mathcal{D}, \tag{14c}$$

$$(13b) - (13j). \tag{14d}$$

where $\mathcal{Z} = \left\{v_c^n, u_d^n, P_c^n, q_d^n, \eta_c, \eta_d\right\}$, $\vartheta = \sum_{c=1}^{C} C_c + \sum_{d=1}^{D} C_d$.

Moreover, the constraints in (13b) and (13c) can be converted into the following form

$$\sum_{n\in\mathcal{N}} R_c^n \geq \exp(\frac{\text{MOS}_{CU_c,min} - C_c}{D}), \forall c \in \mathcal{C} \tag{15}$$

$$\sum_{n\in\mathcal{N}} R_d^n \geq \exp(\frac{\text{MOS}_{D2D_d,min} - C_d}{D}), \forall d \in \mathcal{D}, \tag{16}$$

Besides, we notice that the discrete binary constraints in (13f) and (13h) are difficult to tackle. Thus, we rewrite (13f) and (13h) into the equivalent forms:

$$\sum_{c=1}^{C}\sum_{n=1}^{N} v_c^n - (v_c^n)^2 \leq 0;\ 0 \leq v_c^n \leq 1, \forall c \in \mathcal{C}, \forall n \in \mathcal{N}, \tag{17}$$

$$\sum_{d=1}^{D}\sum_{n=1}^{N} u_d^n - (u_d^n)^2 \leq 0;\ 0 \leq u_d^n \leq 1, \forall d \in \mathcal{D}, \forall n \in \mathcal{N}. \tag{18}$$

Now, the binary variables v_c^n and u_d^n are transformed into continuous variables. By employing penalty method [12], the problem (14) can be further reformulated as

$$\max_{\mathcal{Z}} \sum_{c=1}^{C} D\ln(\eta_c) + \sum_{d=1}^{D} D\ln(\eta_d) + \vartheta - \lambda\varsigma(v_c^n, u_d^n) \tag{19a}$$

$$\text{s.t.} 0 \leq v_c^n \leq 1, \forall c \in \mathcal{C}, \forall n \in \mathcal{N};\ 0 \leq u_d^n \leq 1, \forall d \in \mathcal{D}, \forall n \in \mathcal{N}, \tag{19b}$$

$$(13d) - (13e), (13g), (13i), (13j), (14b) - (14c), (15) - (16), \tag{19c}$$

where $\varsigma(\boldsymbol{v}, \boldsymbol{u}) = \sum_{c=1}^{C}\sum_{n=1}^{N} v_c^n - (v_c^n)^2 + \sum_{d=1}^{D}\sum_{n=1}^{N} u_d^n - (u_d^n)^2$. λ is penalty factor. When λ is sufficiently large, i.e., $\lambda \gg 1$, problem (19) is equivalent to problem (14) [12]. Note that (19) is still a non-convex optimization problem due to the non-convex constraints in (14b)-(14c) and (15)-(16). Next, we propose an efficient two-stage method to optimize subchannel assignment and power allocation separately and alternatively, namely, optimize one while keeping the other fixed, which leads to feasible resource allocation solutions. By decomposing (19) into two subchannel assignment subproblem and power allocation subproblem, the two optimization problems are sequentially carried out, which will be discussed in detail in Subsection III-B and Subsection III-C.

B. Subchannel Assignment optimization

In this subsection, we focus on addressing subchannel allocation subproblem. With given P_c^n and q_d^n, the subchannel allocation subproblem can be formulated as

$$\max_{\mathcal{Z}\backslash\{P_c^n, q_d^n\}} \sum_{c=1}^{C} D\ln(\eta_c) + \sum_{d=1}^{D} D\ln(\eta_d) + \vartheta - \lambda\varsigma(v_c^n, u_d^n) \tag{20a}$$

$$\text{s.t. } (13b) - (13c), (13g), (13i), (13j), (14b) - (14c), (15) - (16), (19b). \tag{20b}$$

One can see that (20) is a non-convex optimization problem, because (14b)-(14c) and (15)-(16) are non-convex. For (14b) and (15), we observe that R_c^n in the left-hand-side (LHS) of the two constraints can be equivalently rewritten into a difference of two concave functions, namely,

$$R_c^n = \overline{R}_c^n - \widetilde{R}_c^n \tag{21}$$

where $\overline{R}_c^n = B_n \log_2\left(|h_c^n|^2 v_c^n p_c^n + I_{c,NOMA}^n + I_{c,D2D}^n + \delta^2\right)$ and $\widetilde{R}_c^n = B_n \log_2\left(I_{c,NOMA}^n + I_{c,D2D}^n + \delta^2\right)$.

Furthermore, we can employ the constrained concave-convex procedure (CCCP) method to handle the non-convex constraints in (14b) and (15). The main idea of CCCP method is to iteratively approximate the second term of R_c^n in (21), i.e., $\widetilde{R}_c^n$, as a linear function by using the first-order Taylor approximation. Specifically, by defining $v_c^{n,r}$ and $u_d^{n,r}$ as the given local point at the rth iteration, the concave function $\widetilde{R}_c^n$ can be upper-bounded by its first-order Taylor expansion [13]. Therefore, we can obtain the following relations

$$\begin{aligned}\widetilde{R}_c^n \leq\ & B_n \log_2\left(I_{c,NOMA}^{n,r} + I_{c,D2D}^{n,r} + \delta^2\right) \\ & + \sum_{\substack{|h_l^n|>|h_c^n| \\ l,c\in\mathcal{C}}} \frac{B_n |h_c^n|^2 p_l^n \log_2(e)\left(v_l^n - v_l^{n,r}\right)}{I_{c,NOMA}^{n,r} + I_{c,D2D}^{n,r} + \delta^2} \\ & + \sum_{d\in\mathcal{D}} \frac{B_n |g_{d,c}^n|^2 q_d^n \log_2(e)\left(u_d^n - u_d^{n,r}\right)}{I_{c,NOMA}^{n,r} + I_{c,D2D}^{n,r} + \delta^2} \triangleq \widetilde{R}_c^{n,up}.\end{aligned} \tag{22}$$

Now $\widetilde{R}_{b,g,n}^{up}$ in (22) is a linear function w.r.t. v_c^n and u_d^n. Replacing $\widetilde{R}_{b,g,n}$ with $\widetilde{R}_{b,g,n}^{up}$, non-convex constraints (14b) and (15) can be converted to the following convex forms

$$\sum_{n\in\mathcal{N}} \overline{R}_c^n - \sum_{n\in\mathcal{N}} \widetilde{R}_c^{n,up} \geq \eta_c, \forall c \in \mathcal{C}, \tag{23}$$

$$\sum_{n\in\mathcal{N}} \overline{R}_c^n - \sum_{n\in\mathcal{N}} \widetilde{R}_c^{n,up} \geq \exp(\frac{\text{MOS}_{CU_c,min} - C_c}{D}), \forall c \in \mathcal{C}. \tag{24}$$

Similarly, the non-convex constraints in (14c) and (16) can also be transformed into the following convex forms

$$\sum_{n\in\mathcal{N}} \overline{R}_d^n - \sum_{n\in\mathcal{N}} \widetilde{R}_d^{n,up} \geq \eta_d, \forall d \in \mathcal{D}, \tag{25}$$

$$\sum_{n\in\mathcal{N}} \overline{R}_d^n - \sum_{n\in\mathcal{N}} \widetilde{R}_d^{n,up} \geq \exp(\frac{\text{MOS}_{D2D_d,min} - C_d}{D}), \forall d \in \mathcal{D}. \tag{26}$$

where $\overline{R}_d^n = B_n \log_2\left(|g_d^n|^2 u_d^n q_d^n + \sum_{c\in\mathcal{C}} |h_{B,d}^n|^2 v_c^n p_c^n + \delta^2\right)$, and $\widetilde{R}_d^{n,up} = B_n \log_2\left(\sum_{c\in\mathcal{C}} |h_{B,d}^n|^2 v_c^{n,r} p_c^n + \delta^2\right) + \sum_{c\in\mathcal{C}} \frac{B_n |h_{B,d}^n|^2 p_c^n \log_2(e)\left(v_c^n - v_c^{n,r}\right)}{|h_{B,d}^n|^2 v_c^{n,r} p_c^n + \delta^2}$.

Finally, based on the transformations in (23)-(26), (20) is converted into the following convex optimization problem

$$\max_{\mathcal{Z}\backslash\{P_c^n, q_d^n\}} \sum_{c=1}^{C} D\ln(\eta_c) + \sum_{d=1}^{D} D\ln(\eta_d) + \vartheta - \lambda\varsigma(v_c^n, u_d^n) \tag{27a}$$

$$\text{s.t. } (13g), (13i), (13j), (19b), (23) - (26), \tag{27b}$$

which can be effectively addressed via advanced convex solver CVX [13].

C. Power Allocation optimization

Once the optimal subchannel assignment solutions v_c^n and u_d^n are obtained for problem (27), we deal with the power allocation subproblem, which can be formulated as

$$\max_{\mathcal{Z}\backslash\{v_c^n,u_d^n\}} \sum_{c=1}^{C} D\ln(\eta_c)+\sum_{d=1}^{D} D\ln(\eta_d)+\vartheta-\lambda\varsigma(v_c^n,u_d^n) \quad (28a)$$

$$\text{s.t. } (13b)-(13e),(13j),(14b)-(14c),(15)-(16). \quad (28b)$$

Since (14b)-(14c) and (15)-(16) are non-convex, problem (28) is a non-convex optimization problem. Let us first tackle (14b) and (15). By leveraging (21), R_c^n in the LHS of (14b) and (15) can be equivalently rewritten into a difference of two concave functions, namely, $R_c^n=\overline{R}_c^n-\widetilde{R}_c^n$. Furthermore, by adopting CCCP method, $\widetilde{R}_c^n$ can be upper-bounded by its first-order Taylor expansion [13]. Specifically, with a given local point at the rth iteration, i.e., $p_c^{n,r}$ and $q_d^{n,r}$, we have

$$\begin{aligned}\widetilde{R}_c^n \le\ & B_n\log_2\left(I_{c,NOMA}^{n,r}+I_{c,D2D}^{n,r}+\delta^2\right)\\ &+\sum_{\substack{|h_l^n|>|h_c^n|\\ l,c\in C}}\frac{B_n|h_c^n|^2v_l^n\log_2(e)\left(p_l^n-p_l^{n,r}\right)}{I_{c,NOMA}^{n,r}+I_{c,D2D}^{n,r}+\delta^2}\\ &+\sum_{d\in\mathcal{D}}\frac{B_n|g_{d,c}^n|^2u_d^n\log_2(e)\left(q_d^n-q_d^{n,r}\right)}{I_{c,NOMA}^{n,r}+I_{c,D2D}^{n,r}+\delta^2}\triangleq\widetilde{R}_c^{n,up}. \quad (29)\end{aligned}$$

One can observe that $\widetilde{R}_c^{n,up}$ in (29) is a linear function w.r.t. p_c^n and q_d^n. Thus, by replacing R_c^n with $\widetilde{R}_c^{n,up}$, (14b) and (15) can be converted to the following convex forms

$$\sum_{n\in\mathcal{N}}\overline{R}_c^n-\sum_{n\in\mathcal{N}}\widetilde{R}_c^{n,up}\ge\eta_c,\forall c\in\mathcal{C}, \quad (30)$$

$$\sum_{n\in\mathcal{N}}\overline{R}_c^n-\sum_{n\in\mathcal{N}}\widetilde{R}_c^{n,up}\ge\exp\left(\frac{\text{MOS}_{CU_c,min}-C_c}{D}\right),\forall c\in\mathcal{C}. \quad (31)$$

Similarly, the non-convex constraints in (14c) and (16) can be transformed into the following convex forms

$$\sum_{n\in\mathcal{N}}\overline{R}_d^n-\sum_{n\in\mathcal{N}}\widetilde{R}_d^{n,up}\ge\eta_d,\forall d\in\mathcal{D}, \quad (32)$$

$$\sum_{n\in\mathcal{N}}\overline{R}_d^n-\sum_{n\in\mathcal{N}}\widetilde{R}_d^{n,up}\ge\exp\left(\frac{\text{MOS}_{D2D_d,min}-C_d}{D}\right),\forall d\in\mathcal{D}. \quad (33)$$

where $\overline{R}_d^n = B_n\log_2\left(|g_d^n|^2u_d^nq_d^n+\sum_{c\in C}|h_{B,d}^n|^2v_c^np_c^n+\delta^2\right)$, and $\widetilde{R}_d^{n,up} = B_n\log_2\left(\sum_{c\in C}|h_{B,d}^n|^2v_c^np_c^{n,r}+\delta^2\right)+\sum_{c\in C}\frac{B_n|h_{B,d}^n|^2v_c^n\log_2(e)\left(p_c^n-p_c^{n,r}\right)}{|h_{B,d}^n|^2v_c^np_c^{n,r}+\delta^2}$.

Finally, with the given local point $p_c^{n,r}$ and $q_d^{n,r}$, and the corresponding convex upper bound functions $\widetilde{R}_c^{n,up}$ and $\widetilde{R}_d^{n,up}$, (28) is reformulated into the following convex optimation problem

$$\max_{\mathcal{Z}\backslash\{v_c^n,u_d^n\}} \sum_{c=1}^{C} D\ln(\eta_c)+\sum_{d=1}^{D} D\ln(\eta_d)+\vartheta-\lambda\varsigma(v_c^n,u_d^n) \quad (34a)$$

$$\text{s.t. } (13b)-(13e),(13j),(30)-(33), \quad (34b)$$

which can be effectively solved via advanced convex solver CVX [13].

IV. Simulation Results

In this section, the performance of the proposed QoE-driven resource allocation scheme in D2D underlaying NOMA cellular network is verified through extensive numerical simulations. The coverage radius the cell is 500 m and the BS is located in the center. The pathloss is model by 148.1 + 37.6$\log_{10}(R)$ dB [7], where R [km] denotes the distance. Small-scale fading of channels are modeled as Rayleigh fading. AWGN spectral density is -174 dBm/Hz. The parameter MSS for web browsing is 1460 bytes [10]. The SC number is $N=10$. The bandwidth of each SC is $B_n=75$ kHz. The number of CUs and D2D pairs are $C=10$ and $D=10$, respectively, and the user satisfaction threshold is $\text{MOS}_{min}=1$, unless otherwise specified. Besides, we assume all users access the web pages with same web page size FS=320 KB [10].

For performance evaluation, the following benchmarks are employed in the simulations: (i) 'CSA + EPA: NOMA': The transmit power from the BS and D2D transmitters is equally allocated to CUs and corresponding D2D receivers, and then CCCP-based SC assignment is performed; (ii) 'RSA + CPA: NOMA': The SCs are randomly assigned to users, and then CCCP-based power allocation is conducted to maximize the sum MOSs; and (iii): 'OMA' scheme. Apart from the above QoE-driven resource allocation benchmarks, we also consider an existing QoS-driven power and SC allocation scheme aiming at maximizing the sum rate of users in a D2D underlaying NOMA cellular network [4], which is termed as (iv): 'QoS-driven resource allocation: NOMA'.

Fig. 2 shows average MOS against the number of CUs with different schemes. The average MOS is defined by the radio of sum MOSs to the total number of users. From Fig. 2, we observe that as the number of CUs increases, the average MOS of the proposed scheme tends to decrease. This is because that although NOMA is employed in the proposed scheme such that multiple CUs can be multiplexed over the same SC, the increase in the number of CUs makes inter-user interference more severe, which degrades the average MOS performance of CUs. Meanwhile, when the number of CUs becomes larger, more SCs will be occupied by the CUs. As a result, the available SCs assigned to D2D users will decrease, which limits the average MOS performance of D2D users. However, as shown in Fig. 2, the proposed NOMA scheme still achieves better user QoE compared with other benchmarks. This is because the proposed scheme derives more efficient power and SC allocation solution toward QoE optimization to both CUs and D2D users, which contributes to better user satisfaction.

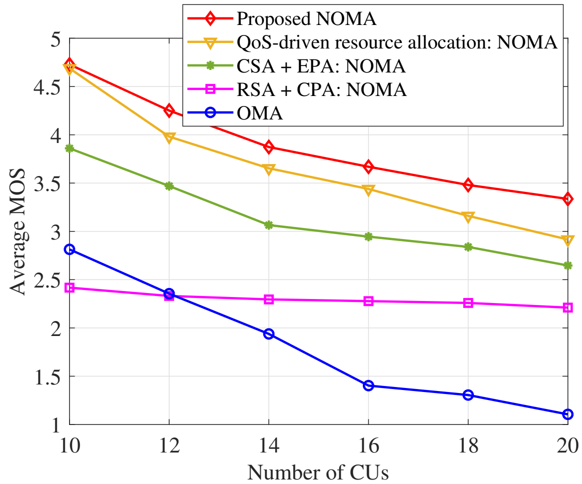

Fig. 2. Average MOS versus the number of CUs with different schemes.

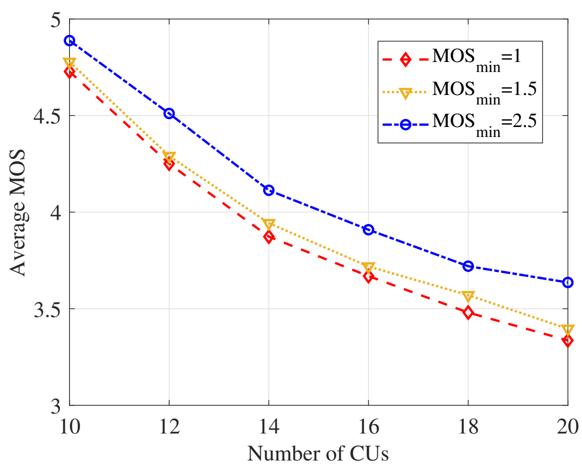

Fig. 3. Average MOS versus versus the number of CUs under different minimum MOS thresholds MOS_{min}.

Particularly, the MOS performance gap between the proposed scheme and QoS-driven resource allocation scheme becomes larger when the number of CUs increases. This means that the QoS-driven resource allocation can not achieve optimal user satisfaction for web browsing service, because QoE is also affected by other non-network-related factors, such as application parameter of the multimedia service.

Fig. 3 depicts average MOS against the number of CUs with different minimum MOS thresholds. From Fig. 3, we find that for different minimum MOS thresholds, i.e., MOS_{min} = 1, 1.5, and 2.5, average MOS tends to decline as the number of CUs increases, which shows similar trends with Fig. 2. Besides, we observe that with MOS_{min} increases, average MOS of proposed scheme tends to increase. This phenomenon illustrates the dependency of QoE-driven optimization algorithm on minimum MOS thresholds, which means that incorporates the QoE threshold mechanism into proposed QoE-driven optimization algorithm could be benefit for enhancing user satisfaction.

V. Conclusion

This paper investigated the QoE-driven power and SC allocation problem in D2D underlaying NOMA cellular networks. A joint optimization problem was formulated, aiming to maximize sum MOSs of all users while ensuring minimum QoE demand of each CU and DU. Since the formulated optimization problem was mixed-integer and non-convex, the original optimization problem was first converted into a more tractable form. Then, by means of AO framework and CCCP technique, a two-stage iteration alogrithm was proposed. Simulation results demonstrated that introducing QoE threshold mechanism into proposed QoE-driven optimization scheme can further improve user satisfaction. Additionally, the results revealed that compared to QoS-driven resource allocation solution, the proposed scheme achieves significant QoE performance enhancement, which characterizes the effectiveness of proposed scheme in optimizing the QoE of CUs and D2D pairs in D2D underlaying NOMA cellular networks.

Acknowledgment

This work was supported by the National Natural Science Foundation of China (NSFC) under Grant 61931005.

References

[1] S. Zhang, J. Liu, H. Guo, M. Qi, and N. Kato, "Envisioning device-to-device communications in 6G," *IEEE Netw.*, vol. 34, no. 3, pp. 86–91, Mar. 2020.

[2] S. Chen, B. Ren, Q. Gao, S. Kang, S. Sun, and K. Niu, "Pattern division multiple accesss–A novel nonorthogonal multiple access for fifth-generation radio networks," *IEEE Trans. Veh. Technol.*, vol. 66, no. 4, pp. 3185–3196, Apr. 2017.

[3] Z. Ding, Y. Liu, J. Choi, Q. Sun, M. Elkashlan, C. I, and H. V. Poor, "Application of non-orthogonal multiple access in LTE and 5G networks," *IEEE Commun. Mag.*, vol. 55, no. 2, pp. 185–191, Feb. 2017.

[4] Y. Pan, C. Pan, Z. Yang, and M. Chen, "Resource allocation for D2D communications underlaying a NOMA-based cellular network," *IEEE Wireless Commun. Lett.*, vol. 7, no. 1, pp. 130–133, Feb. 2018.

[5] Y. Dai, M. Sheng, J. Liu, N. Cheng, X. Shen, and Q. Yang, "Joint mode selection and resource allocation for D2D-enabled NOMA cellular networks," *IEEE Trans. Veh. Technol.*, vol. 68, no. 7, pp. 6721–6733, Jul. 2019.

[6] Y. Jiang, L. Wang, H. Zhao, and H. H. Chen, "Covert communications in D2D underlaying cellular networks with power domain NOMA," *IEEE Syst. J.*, vol. 14, no. 3, pp. 3717–3728, Jun. 2020.

[7] L. Pei, Z. Yang, C. Pan, W. Huang, M. Chen, M. Elkashlan, and A. Nallanathan, "Energy-efficient D2D communications underlaying NOMA-based networks with energy harvesting," *IEEE Commun. Lett.*, vol. 22, no. 5, pp. 914–917, May. 2018.

[8] Z. Ding, Z. Yang, P. Fan, and H. V. Poor, "On the performance of non-orthogonal multiple access in 5G systems with randomly deployed users," *IEEE Signal Process. Lett.*, vol. 21, no. 12, pp. 1501–1505, Dec. 2014.

[9] P. Ameigeiras, J. J. Ramos-Munoz, J. Navarro-Ortiz, P. Mogensen, and J. M. Lopez-Soler, "QoE oriented cross-layer design of a resource allocation algorithm in beyond 3G systems," *Comput. Commun.*, vol. 33, no. 5, pp. 571–582, 2010.

[10] M. Rugelj, U. Sedlar, M. Volk, J. Sterle, M. Hajdinjak, and A. Kos, "Novel cross-layer QoE-aware radio resource allocation algorithms in multiuser OFDMA systems," *IEEE Trans. Commun.*, vol. 62, no. 9, pp. 3196–3208, Sep. 2014.

[11] 3GPP TR 36.912, "Feasibility Study for Further Advancements for E-UTRA (LTE-Advanced) document v11.0.0," *3rd Gen. Partner. Proj., Sophia Antipolis, France, TS36*, Sep. 2012.

[12] D. P. Bertsekas, "Nonlinear programming," *Journal of the Operational Research Society*, vol. 48, no. 3, pp. 334–334, 1997.

[13] S. Boyd and L. Vandenberghe, *Convex optimization*. Cambridge university press, 2004.